

## Open Access Repository eprint

Terms and Conditions: Users may access, download, store, search and print a hard copy of the article. Copying must be limited to making a single printed copy or electronic copies of a reasonable number of individual articles or abstracts. Access is granted for internal research, testing or training purposes or for personal use in accordance with these terms and conditions. Printing for a for-fee-service purpose is prohibited.

Title: Volume determination of the Avogadro spheres of highly enriched  $^{28}\text{Si}$  with a spherical Fizeau interferometer

Author(s): Bartl, G.; Bettin, H.; Krystek, M.; Mai, T.; Nicolaus, A.; Peter, A.

Journal: Metrologia

Year: 2011, Volume: 48, Issue: 2

DOI: doi:10.1088/0026-1394/48/2/S12

Funding programme: iMERA-Plus: Call 2007 SI and Fundamental Metrology

Project title: T1.J1.2: NAH: Avogadro and molar Planck constants for the redefinition of the kilogram

Copyright note: This is an author-created, un-copyedited version of an article accepted for publication in Metrologia. IOP Publishing Ltd is not responsible for any errors or omissions in this version of the manuscript or any version derived from it. The definitive publisher-authenticated version is available online at doi:10.1088/0026-1394/48/2/S12

# Volume determination of the Avogadro spheres of highly enriched $^{28}\text{Si}$ with a spherical Fizeau interferometer

Guido Bartl, Horst Bettin, Michael Krystek, Torsten Mai,  
Arnold Nicolaus, Andreas Peter

Physikalisch-Technische Bundesanstalt (PTB), Bundesallee 100, 38116 Braunschweig,  
Germany

E-mail: [arnold.nicolaus@ptb.de](mailto:arnold.nicolaus@ptb.de)

**Abstract.** Within the scope of the efforts concerning the redefinition of the SI base unit “kg” the final results of the international research project aiming at the redetermination of the Avogadro constant are ready to be announced. Among other quantities the volume of two spheres which are made of a highly enriched  $^{28}\text{Si}$  single crystal had to be determined. For this purpose a special Fizeau interferometer for the measurement of the spheres’ diameters has been developed at PTB. This paper reports the final results of the volumes, the uncertainties and also the latest findings regarding systematic corrections including the effects of surface layers on the pure silicon core. The results are confirmed by density comparison measurements.

PACS numbers: 06.20.Jr, 42.87.Bg, 07.60.Ly, 06.20.-f, 02.60.Ed, 06.30.Dr

Submitted to: *Metrologia*

## 1. Introduction

For a possible new definition of the kilogram the redetermination of the Avogadro constant is one of the most promising ways. For this four parameters are to be measured [1]: molar mass and lattice parameter of a perfect crystal and mass and volume of an artefact, built up from the same crystal. A target relative uncertainty of  $2 \times 10^{-8}$  is to be reached for the entire experiment.

A first set of three spheres was made up of natural silicon consisting of 92.2%  $^{28}\text{Si}$ , 4.7%  $^{29}\text{Si}$  and 3.1%  $^{30}\text{Si}$ . For these spheres an uncertainty of  $3.1 \times 10^{-7}$  was achieved [2]. To further reduce the uncertainty an isotopically nearly pure crystal was fabricated with 99.99%  $^{28}\text{Si}$ , primarily to reduce the uncertainty of the determination of the molar mass. The Institute of Chemistry of High-Purity Substances of the Russian Academy of Sciences (IChHPS RAS) in Nizhny Novgorod and the Central Design Bureau of Machine Building (CDBMB) in Saint Petersburg supplied the enriched material which was grown to a 5 kg mono-crystal in the Leibniz-Institut für Kristallzüchtung (IKZ) Berlin [3]. Cut into ten pieces two parts of the crystal, no. 5 and no. 8, were manufactured at the Australian Centre for Precision Optics (ACPO) to two nearly perfect 1 kg spheres called AVO28-S5 and AVO28-S8. Over the last two years these spheres were subject of detailed and extensive measurements of their mass (BIPM, NMIJ, PTB), volume (NMIJ, PTB) and surface (PTB, NMIJ).

For the determination of the volume of these spheres at PTB a spherical Fizeau interferometer was used, which was developed and tested with measurements of the spheres of natural silicon and which was advanced to reach lowest uncertainties.

This paper describes the measurement setup of the sphere interferometer, explicates the measurement procedure and gives an overview on the data processing. Some new considerations on the measurement uncertainty are discussed and the final results are presented.

## 2. Measurement of the diameter of the spheres

### 2.1. Experimental setup of the spherical Fizeau interferometer

For the volume determination of the silicon spheres a spherical Fizeau interferometer was developed [4]. It consists of a temperature-controlled vacuum chamber and two opposing arms for illuminating and imaging optics. In these optical arms light from a multimode fibre propagates 1.6 m in free space and is then collimated. The plane wave enters the vacuum chamber through an optical window and is subsequently focussed by a Fizeau lens whose focal point is carefully adjusted to the center of the silicon sphere. As the inner surfaces of the two Fizeau lenses are formed concentrically to the focussed wavefront (see figure 1), a spherical etalon is formed in one case, with the sphere removed, between the pair of lenses and in the other case, with the sphere inserted, between the reference face of each lens and the corresponding surface of the sphere. Therefore four measurements are necessary to obtain the diameter of the sphere: the

diameter of the empty etalon  $D$ , which is obtained with the sphere in a lifted position from both sides, and the distances  $d_1$  and  $d_2$  between the sphere and the reference surfaces. The diameter  $d$  of the sphere is then  $d = D - d_1 - d_2$ .

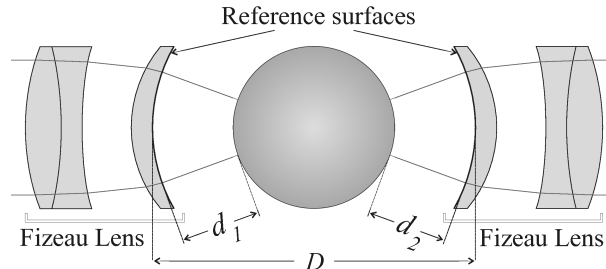


**Figure 1.** Schematic drawing of the central part of the interferometer. The measured quantities are the distances between the sphere surface and the reference surfaces,  $d_1$  and  $d_2$ , and the length of the empty etalon  $D$ .

With this technique 10000 diameter values, only depending on the camera resolution chosen, within a  $60^\circ$  section of the surface can be obtained. To cover the whole sphere with diameter values and to lift it out of the beam path for measuring the length of the empty etalon an elevation and positioning mechanism is used consisting of a liftable column which contains two pairs of plastic wheels as a support for the sphere in the upper position. Lifting and rotation around the vertical axis is done by the column itself and the rotation around the horizontal axis is done by rotation of the wheels. In the measurement position the sphere rests on a three-point support.

To achieve low uncertainties the implementation of a thermal stabilization is a basic prerequisite. In the first instance a laboratory climate control provides temperature fluctuations below 0.1 K in 24 hours. For the second level a pipe network was incorporated in the vacuum chamber housing which is flown-through by a water-glycol-mixture. The temperature of the liquid is stabilized by a thermostat to 0.01 K, so that due to the thermal inertia of the massive body of the vacuum chamber a temperature fluctuation of only a few millikelvin is reached. As the final step the interferometer itself, consisting of a rigid monolithic frame, which contains the Fizeau lenses and the three-point rest of the sphere, is coupled to the vacuum chamber with three small point contacts, so that a weak heat and energy exchange guarantees small temperature fluctuations. For the target uncertainty the temperature of the sphere needs to be measured with an uncertainty of less than 1 mK. To reduce any effects of influencing the temperature of the sphere, thermocouple pairs measure the temperature difference between the sphere and a copper block inside the interferometer frame which acts as a reference body [5]. The temperature of this copper block is measured by common means, i.e. an AC bridge with a  $25 \Omega$  standard platinum resistance thermometer, directly calibrated at the triple point of water and the melting point of gallium.

## 2.2. Measurement procedure

As a preparation of the measurements the sphere to be measured is cleaned with distilled water and Deconex<sup>®</sup> OP 162, a concentrated detergent to remove dust and other particles from the surface. The soap film is then washed up abundantly with water. To remove the final water film threefoldly distilled ethanol is rinsed over the sphere and it is waited until the ethanol is evaporated. Then the sphere is placed on the pair of plastic wheels with the supporting column in the upper position and inserted into the three-point-rest automatically by means of the orientation device. Afterwards the interferometer chamber is closed and slowly evacuated since the Fizeau objectives only allow pressure changes below 100 Pa per second. The final pressure is around 0.3 Pa. Subsequently the optical system is adjusted to the sphere. To obtain the correct position for the optical fiber with relation to the collimator an autocollimation procedure was established. Then each Fizeau lens can be adjusted by three piezo-step-motors to minimize the number of interference fringes in the etalon consisting of the spherical Fizeau surfaces. The autocollimation and fringe reduction adjustment are repeated alternately until both criterions are fulfilled.

For one diameter map four phase maps need to be recorded: the empty etalon from both sides and the gaps between the sphere and the reference surfaces. Each of the phase maps is calculated from five interferograms with phase steps of  $\pi/2$  based on a four-step phase-shifting technique [6, 7]. The phase shift is realized with a tunable laser which is traceable through the comparison with a iodine stabilized He-Ne laser to the SI unit meter [8].

To cover the entire surface of a sphere with measurement points, it is rotated around two perpendicular axes. Since the spheres are tagged according to their crystal orientation with three different marks, a unique and repeatable orientation can be achieved. A typical set of single measurements consists of a sequence of rotation steps between  $15^\circ$  and  $45^\circ$  for both axes. The measurement procedure yields a varying coverage density of measurement values on the surface of the sphere due to overlapping regions of the field of view for different measurement orientations (see figure 2), which has to be taken into account for the evaluation.

## 2.3. Topographies

The described measurement procedure was applied to the two spheres of  $^{28}\text{Si}$ , named AVO28-S5 and AVO28-S8. For the determination of the volume, 32 measurements with different orientations of the respective sphere have been performed for AVO28-S5 and 44 measurements for AVO28-S8. The whole set of measurements gave 320000 and 440000 single diameter values, respectively, distributed all over the sphere and covering the topographies thoroughly. According to [9] the surfaces of the spheres were subdivided into small cells of almost equal area and all measurement values inside a cell were assigned to the center position of this cell. Doing so, a map of the topography and of the distribution of the measuring point densities can be determined, which are shown

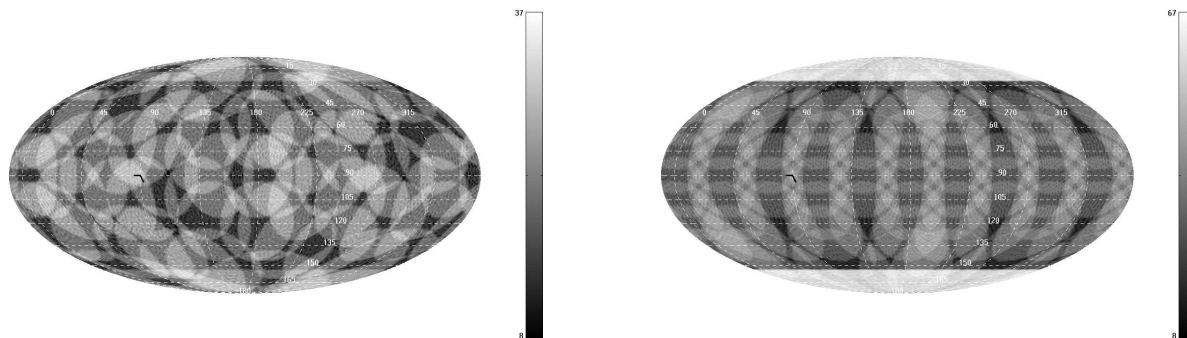


**Figure 2.** Distribution of the measuring positions per graticule cell of the sphere AVO28-S5 (left) and of the sphere AVO28-S8 (right) plotted in Mollweide projection. The greyscales range from 8 to 37 and from 8 to 67 values per graticule cell, respectively.

in the figures 2 and 3 for AVO28-S5 and AVO28-S8.

The color scales are adapted to the respective topography and span 97.8 nm for AVO28-S5 and 89.7 nm for AVO28-S8 related to the diameter variation. The circular structures in figure 2 indicate the shape of the field of view related to one single measurement. Brighter regions indicate a larger amount of measurement values per surface element than darker regions.

Due to the variable coverage density, a mean diameter for the calculation of the volume cannot be obtained simply by taking the average of all single diameter values. This would lead to an overweighted influence of regions with a large amount of diameter values. Instead, a proper method for the determination of the volume is described in section 4.

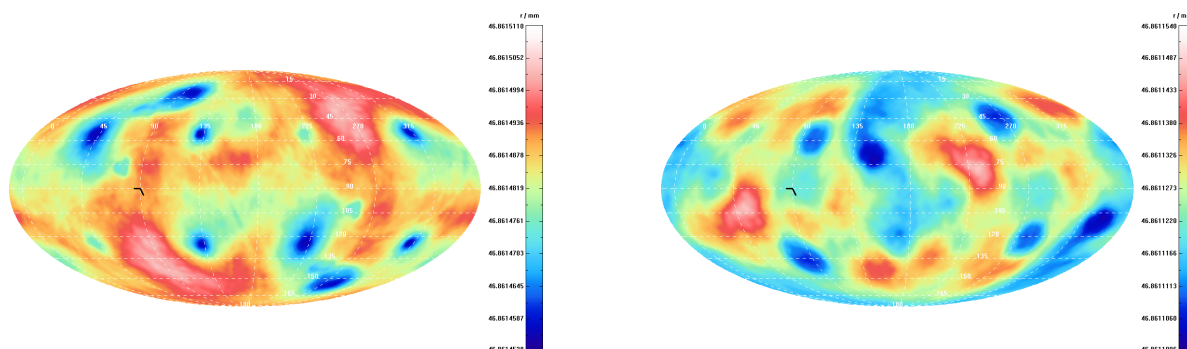


**Figure 3.** Topography of the sphere AVO28-S5 (left) and of the sphere AVO28-S8 (right) plotted in Mollweide projection. The color scales of the topographies span 97.8 nm and 89.7 nm, respectively.

#### 2.4. Systematic corrections

The measurements are influenced by a couple of parameters (see table 1). At first the interferometric influences are to be stated as the intensity measurement of the interferences, the frequencies of the lasers, the precision of the phase steps and an

obliquity correction depending on the size of the fibre exit and the ratio of the focal lengths of the collimator and the Fizeau lens [10]. In order to compensate for the small temperature deviations from 20 °C, we calculate the diameter at 20 °C by using the coefficient of thermal expansion of  $^{28}\text{Si}$  [11]. Two parameters which affect the results depending on the position in the field of view are wave front distortions and parasitic interferences. The latter describe unwanted small interferences between single surfaces of the optical system. They depend on the actual adjustment and occur with varying intensity and location. The wave front distortion comprises global effects as retrace errors [12] due to the shape deviations of both the sphere under test and the reference faces, misalignment and diffraction. Next, each diameter value has to be corrected for the influence of the surface layer on the sphere caused by the phase retardation due to the different optical properties, which needs to be discussed in detail (section 3). Lastly, the sub-item 'volume' collects the contributions which affect the final calculation of the volume. These are uncertainties due to the point coverage of the sphere, possible positioning errors and the goodness of fit.

**Table 1.** Dominating quantities in the uncertainty budgets of the spheres AVO28-S5 and AVO28-S8. The quoted values are standard uncertainties.

Quantity	AVO28-S5	AVO28-S8
	$u(V)/V$ in $10^{-9}$	$u(V)/V$ in $10^{-9}$
Interferometry (Int)	4	4
Temperature (T)	6	6
Wave front distortions (WF)	35	25
Parasitic (Par)	0.2	0.2
Phase change (PC)	5	5
Volume (Vol)	6	6
<b>Total</b>	<b>37</b>	<b>27</b>

Temperature and obliquity correction have to be corrected for their specific value, which is determined by the actual experimental data. On the contrary, all other contributions have the expectation value zero, but certainly contribute to the uncertainty budget. Each correction also contributes to the uncertainty budget.

For the uncertainty of the volume regarding the systematic corrections we have in total:

$$u_{\text{sys}}^2(V) = u_{\text{Int}}^2(V) + u_{\text{T}}^2(V) + u_{\text{Par}}^2(V) + u_{\text{WF}}^2(V) + u_{\text{PC}}^2(V) + u_{\text{Vol}}^2(V)$$

The final uncertainty is presented in section 4.3.

### 3. Considerations on the influence of surface layers

Due to the fact that silicon bodies which are stored in air are covered with oxide layers, their influence on the measurement results needs to be considered. Therefore it is essential to collect information on the composition and the thickness of these surface

layers. Beside the expected silicon-oxide layers Fuchs [13] found metal-silicide (MeSi) layers consisting of copper- and nickel-silicide (table 2). Additionally, a water layer and a layer of longchain hydrocarbons have to be considered. The measurements also show that the composition of these layers (from the inner to the outer layers) lies between  $\text{Si-SiO}_2\text{-MeSi-H}_2\text{O-C}_m\text{H}_n$  and  $\text{Si-MeSi-SiO}_2\text{-H}_2\text{O-C}_m\text{H}_n$ . In the following these configurations are seen as the limit cases of the real layer composition. The calculations are executed for both cases with the assumption of clearly separated layers. The refractive indices and absorption coefficients given in table 2 are valid for thick materials. Due to the lack of knowledge of the optical properties of the layer materials on silicon for ultra-thin films the uncertainties were raised significantly.

**Table 2.** Optical properties of the layers and the silicon core. For some longchain  $\text{C}_m\text{H}_n$  compounds refractive indices at  $\lambda = 589 \text{ nm}$  were found, they differ with chain length and isomerism so that it was useful to assume a mean value and a large uncertainty; for the imaginary part no literature values were found, so that a large uncertainty is assumed, too. For the MeSi-layer the optical properties of NiSi were assumed.

Layer	$n$	$u_n$	$k$	$u_k$	Ref.
$\text{C}_m\text{H}_n$	1.45	0.1	0	0.1	[14]
$\text{H}_2\text{O}$	1.332	0.1	$1.54 \cdot 10^{-8}$	$1 \cdot 10^{-8}$	[15]
$\text{SiO}_2$	1.457	0.1	0	0	[16]
MeSi	2.67	0.20	2.75	0.20	[17]
Si	3.881	0.001	0.019	0.001	[16]

**Table 3.** Thicknesses of the layers for both  $^{28}\text{Si}$  spheres, ordered from the outside to the inside of the sphere.  $t_{\text{SL}}$  is the sum of the layer thicknesses; values in nm.

Layer	$t_{\text{S5}}$	$u_{t,\text{S5}}$	$t_{\text{S8}}$	$u_{t,\text{S8}}$
$\text{C}_m\text{H}_n$	0.54	0.18	0.47	0.16
$\text{H}_2\text{O}$	0.28	0.08	0.28	0.08
$\text{SiO}_2$	1.52	0.20	1.40	0.20
MeSi	0.54	0.16	0.54	0.17
$t_{\text{SL}}$	2.88	0.33	2.69	0.32

To calculate the influence of these layers on the measurement the matrix based method described by Wolf [18] is used. The influence of the interface between the layers  $j$  and  $j + 1$  is described by matrices  $T_{j,j+1}$ :

$$T_{j,j+1} = \frac{1}{t_{j,j+1}} \begin{pmatrix} 1 & r_{j,j+1} \\ r_{j,j+1} & 1 \end{pmatrix}, \quad (2)$$

where  $t_{j,j+1}$  and  $r_{j,j+1}$  are the complex coefficients of transmission and reflection. In the present case, i.e. for perpendicular incidence, one gets according to [19]

$$r_{j,j+1} = \frac{\tilde{n}_j - \tilde{n}_{j+1}}{\tilde{n}_j + \tilde{n}_{j+1}} \quad (3)$$

$$t_{j,j+1} = \frac{2\tilde{n}_j}{\tilde{n}_j + \tilde{n}_{j+1}} \quad (4)$$

with  $\tilde{n}_i$  as the refractive index of the  $i$ -th layer. The influence of the layer  $j$  is described

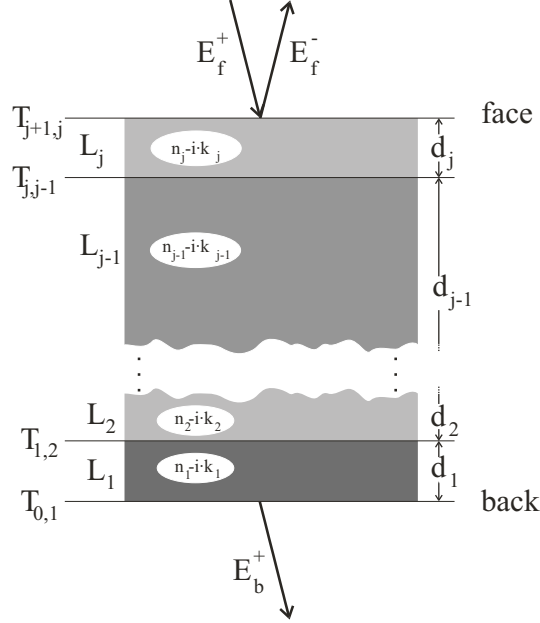


**Figure 4.** Assumed layer model for the calculation of the total reflection coefficient.

by matrix  $L_j$ , which is in the case of perpendicular incidence

$$L_j = \begin{pmatrix} \exp\left(i \cdot \frac{2\pi d_j \tilde{n}_j}{\lambda}\right) & 0 \\ 0 & \exp\left(-i \cdot \frac{2\pi d_j \tilde{n}_j}{\lambda}\right) \end{pmatrix}. \quad (5)$$

The properties of a layer system consisting of  $n$  layers can now be expressed as

$$S = T_{n,n+1} \cdot L_n \cdot T_{n-1,n} \cdot \dots \cdot L_1 \cdot T_{0,1}, \quad (6)$$

where the layers  $n + 1$  and  $0$  are the substrate or the surrounding medium. With this matrix  $S$  the relation between the electrical fields of the input wave  $E_f^+$ , the reflected wave  $E_f^-$  and the transmitted wave  $E_b^+$  can be written as

$$\begin{pmatrix} E_f^+ \\ E_f^- \end{pmatrix} = S \cdot \begin{pmatrix} E_b^+ \\ 0 \end{pmatrix} = \begin{pmatrix} S_{11} & S_{12} \\ S_{21} & S_{22} \end{pmatrix} \cdot \begin{pmatrix} E_b^+ \\ 0 \end{pmatrix} \quad (7)$$

so that the complex reflection factor  $r_{\text{system}}$  of the entire layer system is

$$r_{\text{system}} = \frac{E_f^-}{E_f^+} = \frac{S_{21}}{S_{11}}. \quad (8)$$

The phase shift between the incident and the reflected wave can then be calculated by

$$\phi = \arctan \left( \frac{\text{Im}(r_{\text{system}})}{\text{Re}(r_{\text{system}})} \right). \quad (9)$$

If the wave would be reflected by an ideal and non-absorbing medium, the phase shift would amount to  $\pi$ , so that for the deviation in the measured radius follows:

$$\Delta r = \frac{\pi - \phi}{2\pi} \lambda \cdot \frac{1}{2}. \quad (10)$$

The last factor originates from the way of the wave back and forth. The measurement correction of the diameter of the inner, pure silicon core due to the surface layers is then

$$\Delta d = 2 \Delta r - 2 t_{\text{SL}}. \quad (11)$$

### 3.1. Uncertainty estimation

For further evaluation the overall uncertainty following from the uncertainties of the single layer properties was calculated. Therefore a Monte Carlo Method (MCM) fulfilling the requirements of the GUM-supplement 1 [20] was implemented. In this MCM for every quantity an array was created with  $10^7$  values distributed normally in a random order around the nominal value and with a standard deviation which equals the denoted uncertainty of the respective quantity. With the array index counting for all of the  $10^7$  combinations the resulting phase shift was calculated. Afterwards a histogram with 4000 intervals between the maximum and the minimum value from the calculations was filled with the results. Due to the fact that there was still some scatter in the histogram, a Gaussian function was fitted to the data so that the center point and the standard deviation which can be interpreted as the uncertainty were obtained.

### 3.2. Results

The diameter corrections resulting from the optical effects of the surface layers are shown in table 4. The phase correction uncertainty  $u_{\text{PC}}(V)$ , i.e. related to the volume, is already stated in table 1. For these values the most contributing factors are the uncertainties of the optical constants, especially of the MeSi layer. Due to the lack of knowledge of the real composition of the surface layers both models are combined resulting in the mean value and the combined uncertainty.

**Table 4.** Correction terms for the diameter measurements of the  $^{28}\text{Si}$  spheres AVO28-S5 and AVO28-S8.

<b>Configuration</b>	$\Delta d_{\text{PC,S5}}/\text{nm}$	$\Delta d_{\text{PC,S8}}/\text{nm}$
Si-SiO <sub>2</sub> -MeSi-H <sub>2</sub> O-C <sub>m</sub> H <sub>n</sub>	0.13(15)	0.09(15)
Si-MeSi-SiO <sub>2</sub> -H <sub>2</sub> O-C <sub>m</sub> H <sub>n</sub>	0.00(14)	-0.03(14)
<b>Mean of both models</b>	<b>0.07(15)</b>	<b>0.03(15)</b>

## 4. Volume determination

### 4.1. Parameterization of the topography

For the calculation of the volume based on the point cloud of diameter values, it is convenient to parameterize the topography of the sphere by real spherical harmonics which are defined as follows:

$$Y_{\ell m}(\vartheta, \varphi) = \begin{cases} \frac{1}{\sqrt{2}} (Y_{\ell}^m + (-1)^m Y_{\ell}^{-m}) & \text{for } m > 0 \\ Y_{\ell}^0 & \text{for } m = 0 \\ \frac{1}{i\sqrt{2}} (Y_{\ell}^{-m} - (-1)^m Y_{\ell}^m) & \text{for } m < 0 \end{cases} \quad (12)$$

$$= \begin{cases} \sqrt{2} N_{\ell, m} P_{\ell}^m(\cos \vartheta) \cos(m\varphi) & \text{for } m > 0 \\ N_{\ell, 0} P_{\ell}^0(\cos \vartheta) & \text{for } m = 0 \\ \sqrt{2} N_{\ell, -m} P_{\ell}^{-m}(\cos \vartheta) \sin(-m\varphi) & \text{for } m < 0 \end{cases} , \quad (13)$$

where  $\ell \in \mathbb{N}$ ,  $m \in \{-\ell, -\ell+1, \dots, \ell\}$ ,  $(\vartheta, \varphi)$  are spherical coordinates,  $Y_{\ell}^m$  are spherical harmonics as defined in [21] with the normalization coefficient  $N_{\ell, m}$  and  $P_{\ell}^m(\cos \vartheta)$  are associated Legendre functions. The parameterization of the topography is then given by the expression

$$R(\vartheta, \varphi) = \sum_{\ell=0}^{\infty} \sum_{m=-\ell}^{\ell} c_{\ell m} Y_{\ell m}(\vartheta, \varphi) , \quad (14)$$

which is in practice limited to a number of  $N$  coefficients  $c_{\ell m}$  with the constraint  $N = (\ell_{\max} + 1)^2$ . These coefficients are determined by a linear least squares optimization based on the data set of the diameter values analogously to [22, 23].

Then the volume of the sphere can be calculated by integration over the full solid angle:

$$V = \int_0^{\pi} \int_0^{2\pi} \int_0^{R(\vartheta, \varphi)} r^2 \sin \vartheta \, dr \, d\varphi \, d\vartheta \quad (15)$$

$$= \frac{1}{3} \int_0^{\pi} \int_0^{2\pi} [R(\vartheta, \varphi)]^3 \sin \vartheta \, d\varphi \, d\vartheta . \quad (16)$$

Rewriting the double sum in Equation (14) to  $\sum_{i=0}^{N-1} c_i Y_i(\vartheta, \varphi)$  with  $i = \ell(\ell + 1) + m$  ( $j$  and  $k$  analogously) yields

$$V = \frac{1}{3} \sum_{i=0}^{N-1} \sum_{j=0}^{N-1} \sum_{k=0}^{N-1} c_i c_j c_k \mathcal{I}_{i,j,k}(\vartheta, \varphi) , \quad (17)$$

where

$$\mathcal{I}_{i,j,k}(\vartheta, \varphi) = \int_0^{\pi} \int_0^{2\pi} Y_i(\vartheta, \varphi) Y_j(\vartheta, \varphi) Y_k(\vartheta, \varphi) \sin \vartheta \, d\varphi \, d\vartheta . \quad (18)$$

Hence, it is sufficient to know the coefficients  $c_{lm}$  from the least squares fit and the results of the integrals  $\mathcal{I}_{i,j,k}(\vartheta, \varphi)$  for the evaluation of the triple sum in Equation (17) to get the volume  $V$ . The solution of the integral over the triple product of the real spherical harmonics is briefly outlined in the appendix.

#### 4.2. Calculation of the uncertainty

Besides the uncertainties of the systematic corrections from Equation (1) the statistical uncertainty of the least squares optimization has to be taken into account. In total the uncertainty of the volume  $u(V)$  reads

$$u^2(V) = u_{\text{stat}}^2(V) + u_{\text{syst}}^2(V). \quad (19)$$

According to the GUM  $u_{\text{stat}}^2(V)$  can be derived from Equation (17) [24, 25]. Thus, we have the expression for the uncertainty of correlated quantities:

$$u_{\text{stat}}^2(V) = \sum_{i=0}^{N-1} \left( \frac{\partial V}{\partial c_i} \right)^2 u^2(c_i) + 2 \cdot \sum_{i=0}^{(N-1)-1} \sum_{j=i+1}^{N-1} \frac{\partial V}{\partial c_i} \frac{\partial V}{\partial c_j} u(c_i, c_j). \quad (20)$$

Since the covariance matrix is computed by the fit algorithm [23],  $u(c_i)$  and  $u(c_i, c_j)$  are already known. The sensitivity coefficients are calculated analogously to the following example for the  $n$ -th coefficient:

$$\frac{\partial V}{\partial c_n} = \frac{1}{3} \sum_{i=0}^{N-1} \sum_{j=0}^{N-1} \sum_{k=0}^{N-1} \frac{\partial}{\partial c_n} c_i c_j c_k \mathcal{I}_{i,j,k}(\vartheta, \varphi) \quad (21)$$

$$= \sum_{i=0}^{N-1} c_i^2 \mathcal{I}_{i,i,n}(\vartheta, \varphi) + 2 \cdot \sum_{i=0}^{(N-1)-1} \sum_{j=i+1}^{N-1} c_i c_j \mathcal{I}_{i,j,n}(\vartheta, \varphi). \quad (22)$$

#### 4.3. Final results

By use of Equation (17) the volume is calculated on the basis of the data sets shown in the figures 2 and 3. For both of the spheres, AVO28-S5 and AVO28-S8, the calculation from section 4.2 yields a relative uncertainty of the statistical contribution  $u_{\text{stat}}(V)/V$  in the order of  $10^{-10}$  and can thus be neglected. Therefore, the uncertainty is dominated by the systematic effects specified in section 2.4 with the values from table 1:

$$u^2(V) \approx u_{\text{syst}}^2(V). \quad (23)$$

The pure silicon core volumes and their uncertainties are as follows:

$$V_{\text{AVO28-S5}} = 431059.0566(158) \text{ mm}^3 \quad (24)$$

and

$$V_{\text{AVO28-S8}} = 431049.1131(117) \text{ mm}^3. \quad (25)$$

This corresponds to a mean diameter of

$$d_{\text{AVO28-S5}} = 93.7229717(11) \text{ mm} \quad (26)$$

and

$$d_{\text{AVO28-S8}} = 93.7222511(9) \text{ mm}, \quad (27)$$

respectively. These results apply for a temperature of 20 °C and a pressure of 0 Pa.

## 5. Linking the measurements

Although results with low uncertainties are available from the measurements of the spheres, one aspect of the determination of Avogadro's constant, in particular the determination of the macroscopic density, offers the advantage to compare the results of the spheres. The density  $\rho = m/V$  of the whole sphere can be calculated from the mean core diameter and the mean surface layer thickness  $t_{\text{SL}}$  – resulting in the volume  $V$  of the whole sphere – and the mass  $m$  of the sphere determined by mass comparison to mass standards which are traceable to the International Kilogram Prototype [26] (see table 5).

**Table 5.** Density determination of the enriched silicon spheres (including the surface layer) using the PTB diameter measurements.

Sphere	Mean core diameter $d/\mu\text{m}$	$t_{\text{SL}}/\text{nm}$	Mass $m/\text{kg}$	Density $\rho/\text{kg}/\text{m}^3$
AVO28-S5	93722.9717(11)	2.88(33)	1.0000877724(41)	2320.070936(96)
AVO28-S8	93722.2511(9)	2.69(32)	1.0000647307(41)	2320.071025(83)

Taking into account the correlations of the measurements, a density difference of the spheres of 0.000 089(97) kg/m<sup>3</sup> or 38(42) × 10<sup>-9</sup>, relatively, is yielded. These calculated densities of the whole spheres can be checked by a direct density comparison of the two spheres as can be performed with high precision by the pressure-of-flotation method [27, 28]. In this method each of the silicon samples floats freely in a suitable liquid that has the same density as silicon. Fine adjustment of the liquid density is achieved by small pressure changes, at NMIJ by means of a pressure controller and at PTB by the hydrostatic pressure produced by a liquid column, the height of which can be changed by moving an additional vessel connected to the main measuring vessel (containing the samples). The  $^{28}\text{Si}$  spheres have nearly the same density, thus NMIJ used exceptionally the same pressure for both spheres floating simultaneously and measured the height difference of the spheres in the vessel, resulting in  $\Delta\rho/\rho = 26(9) \times 10^{-9}$  [29]. At PTB, the usual procedure was used, i. e., the spheres floated subsequently at the same height but at different controlled pressures, yielding  $\Delta\rho/\rho = 20(10) \times 10^{-9}$ . Both density difference measurements agree with each other and with the above calculated density difference within the stated uncertainties.

## 6. Conclusion

Although being expected to yield the highest contribution to the uncertainty of the Avogadro constant, the determination of the volume of silicon spheres which range in the decimeter-region reaches an uncertainty below one nanometer. This was enabled by the development of a specifically designed interferometer combined with modern mathematical methods.

The interferometer bases on spherical wavefronts which are adopted to the shape of a sphere and therefore reduce the influence of optical corrections. The optical design of the interferometer allows a high number of diameters to be measured at the same time facilitating  $60^\circ$ -topographies of the sphere. A precise orientating device together with a specific mathematical model enables the complete topography and guarantees a correct weighting of the measured data. The volume is then calculated by integrating the parameterized topography.

The uncertainty can be determined for the different contributions in detail and is validated by experimental data or theoretical considerations. In the present case, as the spheres are contaminated with nickel and copper, the surface layer model is strongly affected by the lack of information about the consistence of the metal components and their distribution. This is taken into account by a considerable uncertainty. On the other hand that causes reasonable hopes that the already started reduction of the contamination will reduce the uncertainty perspicuously.

Finally, valuable evidence for plausibility and coherence is shown by a comparison between direct density comparisons and the results from mass and volume measurements.

## Acknowledgement

This research received funds from the European Community's 7th Framework Programme ERA-NET Plus (grant 217257) and the International Science and Technology Center (grant 2630).

## Appendix A. Integral over the triple product of real spherical harmonics

The integral in Equation (18) can be separated into three parts by use of the definition of the  $Y_{\ell m}(\vartheta, \varphi)$ . The first part is a product of the normalisation coefficients and the second one is an integral over  $\varphi$ , where the integrand is a product of three sines or cosines, which can be calculated easily. The third part is an integral over  $\vartheta$ , where the integrand is a triple product of associated Legendre polynomials and  $\sin \vartheta$ . By use of the substitution  $\xi = \cos \vartheta$  this can be written as

$$\mathcal{G}(\ell_i, \ell_j, \ell_k, m_i, m_j, m_k) = \int_{-1}^{+1} P_{\ell_i}^{m_i}(\xi) P_{\ell_j}^{m_j}(\xi) P_{\ell_k}^{m_k}(\xi) d\xi \quad (\text{A.1})$$

This integral is basically known in literature [30] as Gaunt's Integral or Gaunt Coefficient and is frequently used in quantum mechanical calculation. In the present case, however, we also have to take into account the combinations of  $i$ ,  $j$  and  $k$ , which are neglected for physical reasons in the field of quantum mechanics. Thus the integral (A.1) has to be evaluated explicitly. Using Rodrigues' representation of the Legendre polynomials [31], we find after a somewhat lengthy calculation the solution

$$\mathcal{G}(\ell_i, \ell_j, \ell_k, m_i, m_j, m_k) = A \sum_{\substack{j_1=0 \\ 2j_1 \geq \ell_i + m_i}}^{\ell_i} \sum_{\substack{j_2=0 \\ 2j_2 \geq \ell_j + m_j}}^{\ell_j} \sum_{\substack{j_3=0 \\ 2j_3 \geq \ell_k + m_k}}^{\ell_k} B_J C_{j_1 j_2 j_3}$$

with the abbreviations

$$A = \frac{1 + (-1)^{L+M}}{2^{L+1}} \frac{(\ell_i + m_i)! (\ell_j + m_j)! (\ell_k + m_k)!}{\ell_i! \ell_j! \ell_k!},$$

$$B_J = (-1)^J \frac{\Gamma\left(\frac{M}{2} + 1\right) \Gamma\left(\frac{2J - (L + M) + 1}{2}\right)}{\Gamma\left(\frac{2J - L + 1}{2} + 1\right)},$$

$$C_{j_1 j_2 j_3} = \binom{\ell_i}{j_1} \binom{2j_1}{\ell_i + m_i} \binom{\ell_j}{j_2} \binom{2j_2}{\ell_j + m_j} \binom{\ell_k}{j_3} \binom{2j_3}{\ell_k + m_k},$$

$$L = \ell_i + \ell_j + \ell_k, \quad M = m_i + m_j + m_k, \quad J = j_1 + j_2 + j_3.$$

As can be seen, the integral vanishes, unless  $L + M$  is an even integer. However, since from the integral over  $\varphi$  it already follows that  $M$  must be an even integer, we conclude that  $L$  must also be an even integer and the coefficients  $B_j$  are rational numbers. Thus, any integral over a triple product of associated Legendre polynomials can be calculated exactly, yielding either zero or a rational number.

## References

- [1] B. Andreas, Y. Azuma, G. Bartl, P. Becker, H. Bettin, M. Borys, I. Busch, P. Fuchs, K. Fujii, H. Fujimoto, E. Kessler, M. Krumrey, U. Kuetgens, N. Kuramoto, G. Mana, E. Massa, S. Mizushima, A. Nicolaus, A. Picard, A. Pramann, O. Rienitz, D. Schiel, S. Valkiers, A. Waseda, and S. Zakel. Counting the atoms in a  $^{28}\text{Si}$  crystal for a new kilogram definition. *Metrologia*, 2011.
- [2] K. Fujii, A. Waseda, N. Kuramoto, S. Mizushima, P. Becker, H. Bettin, A. Nicolaus, U. Kuetgens, S. Valkiers, P. Taylor, P. de Bièvre, G. Mana, E. Massa, R. Matyi, Jr. E. G. Kessler, and M. Hanke. Present State of the Avogadro Constant Determination From Silicon Crystals With Natural Isotopic Compositions. *IEEE Trans. Instrum. Meas.*, 54(2):854–859, April 2005.
- [3] P. Becker, D. Schiel, H.-J. Pohl, A. K. Kaliteevski, O. N. Godisov, M. F. Churbanov, G. G. Devyatikh, A. V. Gusev, A. D. Bulanov, S. A. Adamchik, V. A. Gavva, I. D. Kovalev, N. V. Abrosimov, B. Hallmann-Seiffert, H. Riemann, S. Valkiers, P. Taylor, P. De Bièvre, and E. M. Dianov. Large-scale production of highly enriched  $^{28}\text{Si}$  for the precise determination of the Avogadro constant. *Meas. Sci. Technol.*, 17:1854–1860, 2006.

- [4] R. A. Nicolaus, G. Bönsch, and C.-S. Kang. Interferometrische Kalibrierverfahren für die Schrittweitensteuerung eines Phasenverschiebeinterferometers. *Technisches Messen*, 67:328–333, Juli/August 2000.
- [5] R. A. Nicolaus and R. D. Geckeler. Improving the Measurement of the Diameter of Si Spheres. *IEEE Trans. Instrum. Meas.*, 56(2):517–522, April 2007.
- [6] G. Bönsch and H. Böhme. Phase-determination of Fizeau interferences by phase-shifting interferometry. *Optik*, 82(4):161–164, 1989.
- [7] R. A. Nicolaus and G. Bönsch. Absolute volume determination of a silicon sphere with the spherical interferometer of PTB. *Metrologia*, 42:24–31, Januar 2005.
- [8] R. A. Nicolaus, G. Bartl, and A. Peter. Interferometrie an Kugeln. *PTB-Mitteilungen*, 120(1):23–30, 2010.
- [9] G. Bartl and A. Nicolaus. Influence of the distribution of measuring points on the mean diameter determination of the Avogadro project’s silicon spheres. *Meas. Sci. Technol.*, 20:065104 (6pp), 2009.
- [10] R. A. Nicolaus and G. Bönsch. Aperture correction for a sphere interferometer. *Metrologia*, 46:668–673, 2009.
- [11] G. Bartl, A. Nicolaus, E. Kessler, R. Schödel, and P. Becker. The coefficient of thermal expansion of highly enriched  $^{28}\text{Si}$ . *Metrologia*, 46:416–422, 2009.
- [12] D. Malacara. *Optical Shop Testing*, chapter Interferometer Optical Errors, pages 611–612. Pure and Applied Optics. John Wiley & Sons, Inc., 3rd edition edition, 2007.
- [13] I. Busch, Y. Azuma, H. Bettin, L. Cibik, P. Fuchs, K. Fujii, M. Krumrey, U. Kuetgens, N. Kuramoto, and S. Mizushima. Surface layer determination for the Si spheres of the Avogadro project. *Metrologia*, accepted.
- [14] Ch. Wohlfarth and B. Wohlfarth. *Refractive Indices of Organic Liquids*, volume 38b of *Landolt-Börnstein, Group 3*. 1996.
- [15] E. D. Palik. *Handbook of optical constants of solids, Vol. 2*. Academic Press, Inc., reprint edition, 2003.
- [16] E. D. Palik. *Handbook of optical constants of solids, Vol. 1*. Academic Press, Inc., 6. reprint edition, 2004.
- [17] M. Amiotti, A. Borghesi, G. Guizzetti, and F. Nava. Optical properties of polycrystalline nickel silicides. *Physical Review B*, 42, Number 14:8939–8946, 1990.
- [18] A. Wolf. *Modifikation der Lichtausbreitung in Halbleitern durch photogenerierte Ladungsträger*. PhD thesis, Technische Universität Carolo-Wilhelmina zu Braunschweig, Germany, 1993.
- [19] L. Bergmann and C. Schaefer. *Optics of waves and particles*. De Gruyter, 1999.
- [20] Joint Committee for Guides in Metrology. Evaluation of measurement data – Supplement 1 to the ‘Guide to the expression of uncertainty in measurement’ – Propagation of distributions using a Monte Carlo method, September 2008.
- [21] C. Cohen-Tannoudji, B. Diu, and F. Laloé. *Quantum Mechanics – Part 1*. Wiley, 1977.
- [22] W. J. Giardino and G. Mana. Sphericity analysis of solid density standards. *Rev. Sci. Instrum.*, 69(3):1383–1390, March 1998.
- [23] G. Bartl, M. Krystek, R. A. Nicolaus, and W. Giardino. Interferometric determination of the topographies of absolute sphere radii using the sphere interferometer of PTB. *Measurement Science and Technology*, 21(11):115101, 2010.
- [24] Joint Committee for Guides in Metrology. Evaluation of measurement data – Guide to the expression of uncertainty in measurement, September 2008.
- [25] ISO. *Guide to the expression of uncertainty in measurement*. International organization for standardization, Genève, Switzerland, first edition, reprinted 1995 edition, 1993.
- [26] A. Picard, P. Barat, M. Borys, M. Firlus, and S. Mizushima. State-of-the-art mass determination of  $^{28}\text{Si}$  spheres for the Avogadro project. *Metrologia*, submitted.
- [27] H. Bettin and H. Toth. Solid density determination by the pressure-of-flotation method. *Meas. Sci. Technol.*, 17:2567–2573, 2006.

- [28] A. Waseda and K. Fujii. Density comparison measurements of silicon crystals by a pressure-of-flotation method at NMIJ. *Metrologia*, 41:S62–S67, 2004.
- [29] A. Waseda and K. Fujii. Density comparison of isotopically purified silicon single crystals by the pressure-of-flotation method. *IEEE Trans. Instrum. Meas.*, accepted for publication.
- [30] J. A. Gaunt. The triplets of helium. *Phil. Trans. R. Soc. Lond. A*, 228:151–196, 1929.
- [31] B. O. Rodrigues. Mémoire sur l’attraction des sphéroïdes. *Correspondance sur l’école roy. pol.*, III:361–385, 1816.